# Proceedings of
# FEniCS 2021
## 22–26 March 2021


**Editors**

Igor Baratta

Jørgen S. Dokken

Chris Richardson

Matthew W. Scroggs

# Plasma modelling using FEniCS and FEDM

**Aleksandar P. Jovanovic**, Leibniz Institute for Plasma Science and Technology (INP), Germany
Detlef Loffhagen, Leibniz Institute for Plasma Science and Technology (INP), Germany
Markus M. Becker, Leibniz Institute for Plasma Science and Technology (INP), Germany

**25 March 2021**

Non-thermal low-temperature plasmas produced by electric discharges are widely used for various kinds of applications, such as chemical processing (like ozone generation), surface processing (such as plasma etching and sputtering), plasma actuators, or biomedical applications. In order to determine the governing physical and chemical processes, which is sometimes ambitious by experimental methods, plasma modelling is an additional option to be applied. For the numerical analysis of atmospheric-pressure plasmas, which are considered here, fluid models are mostly used due to their computational efficiency. Common fluid models for non-thermal plasmas consist of a set of balance equations for the particle number densities of the relevant plasma species and the energy density of electrons. Poisson's equation is typically solved to self-consistently calculate the electric potential and field. Depending on the gas under consideration the number of species that needs to be taken into account spans from tens to hundreds, which results in the same number of balance equations that need to be solved. At the same time, the number of collision and radiation processes to be considered can even reach thousands, which can make setting-up of the model difficult. Moreover, the physical time scales in plasmas range from picoseconds (electron kinetics) to tens of seconds (slow plasma-chemical reactions) so that the implementation of adaptive time stepping methods is necessary. The present FEniCS-based FEDM (Finite Element Discharge Modelling) code addresses these challenges by automating the model set-up procedure and implementing a backward differentiation formula for time stepping. This contribution represents the main features of the code, shows results of verification studies using benchmarking, and highlights how FEniCS can be used for the numerical analysis of dielectric barrier discharges in argon at atmospheric pressure.

The present work was funded by the Deutsche Forschungsgemeinschaft – project number 407462159.

You can cite this talk as:

Aleksandar P. Jovanovic, Detlef Loffhagen, and Markus M. Becker. "Plasma modelling using FEniCS and FEDM". In: *Proceedings of FEniCS 2021, online, 22–26 March* (eds Igor Baratta, Jørgen S. Dokken, Chris Richardson, Matthew W. Scroggs) (2021), 577–597. DOI: 10.6084/m9.figshare.14495562.

BibTeX for this citation can be found at https://mscroggs.github.io/fenics2021/talks/jovanovic.html.

# Plasma modelling using FEniCS and FEDM

A. P. Jovanović, D. Loffhagen, and M. M. Becker

Leibniz Institute for Plasma Science and Technology (INP)
Felix-Hausdorff-Str. 2, 17489 Greifswald

*FEniCS 2021*
*25 March 2021*

Funded by the Deutsche Forschungsgemeinschaft - project number 407462159

FROM IDEA TO PROTOTYPE

# Introduction

- Plasma is a gaseous state in which free electrons and ionised atoms or molecules exist.
- Non-thermal low-temperature plasmas considered here are usually produced by electric discharges.
- They are used for different applications, such as chemical and surface processing, or biomedical applications.
- In order to describe physical and chemical processes in plasma, experimental studies are often supplemented by numerical modelling.

*Images obtained from https://www.inp-greifswald.de/*

# Introduction

- Plasma is a gaseous state in which free electrons and ionised atoms or molecules exist.
- Non-thermal low-temperature plasmas considered here are usually produced by electric discharges.
- They are used for different applications, such as chemical and surface processing, or biomedical applications.
- In order to describe physical and chemical processes in plasma, experimental studies are often supplemented by numerical modelling.

*Images obtained from https://www.inp-greifswald.de/*

# Introduction

- Plasma is a gaseous state in which free electrons and ionised atoms or molecules exist.
- Non-thermal low-temperature plasmas considered here are usually produced by electric discharges.
- They are used for different applications, such as chemical and surface processing, or biomedical applications.
- In order to describe physical and chemical processes in plasma, experimental studies are often supplemented by numerical modelling.

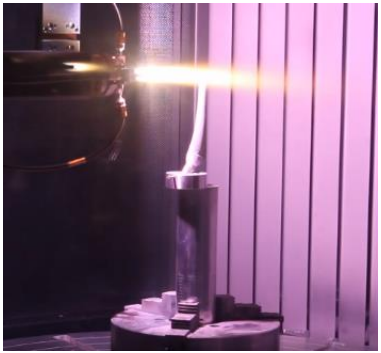

*Images obtained from https://www.inp-greifswald.de/*

# Introduction

- Plasma is a gaseous state in which free electrons and ionised atoms or molecules exist.
- Non-thermal low-temperature plasmas considered here are usually produced by electric discharges.
- They are used for different applications, such as chemical and surface processing, or biomedical applications.
- In order to describe physical and chemical processes in plasma, experimental studies are often supplemented by numerical modelling.

*Images obtained from https://www.inp-greifswald.de/*

# Governing equations

- Poisson's equation for electric potential

$$-\varepsilon_0\varepsilon_r\nabla^2\phi = \sum_p q_p n_p$$
$$\mathbf{E} = -\nabla\phi$$

- Electron energy balance equation

$$\frac{\partial w_e}{\partial t} + \nabla\cdot\mathbf{Q}_e = -e_0\mathbf{E}\cdot\mathbf{\Gamma}_e + \widetilde{S}_e$$
$$\mathbf{Q}_e = -\tfrac{5}{3}b_e\mathbf{E}w_e - \nabla(\tfrac{5}{3}D_e w_e)$$
$$\widetilde{S}_e = \sum_{j=1}^{N_r}\Delta\varepsilon_j R_j$$

- Continuity equation for particle densities

$$\frac{\partial n_p}{\partial t} + \nabla\cdot\mathbf{\Gamma}_p = S_p$$
$$\mathbf{\Gamma}_p = \mathrm{sgn}(q_p)b_p\mathbf{E}n_p - \nabla(D_p n_p)$$
$$S_p = \sum_{j=1}^{N_r}(G_{pj} - L_{pj})k_j\prod_{i=1}^{N_s} n_i^{\beta_{ij}}$$

- In order to solve the equations, appropriate set of boundary conditions is used:
  - Dirichlet and Robin boundary conditions for Poisson's equation
  - Robin boundary conditions for continuity equations, and electron energy balance equation.

*M. M. Becker et al., J. Phys. D: Appl. Phys.* ***46*** *(2013) 355203*
*G. J. M. Hagelaar et al., Phys. Rev. E* ***62*** *(2000) 1452*

# Challenges in plasma modelling

- For appropriate description of the processes in plasma, lots of particles, and consequently, lots of processes need to be taken into account.

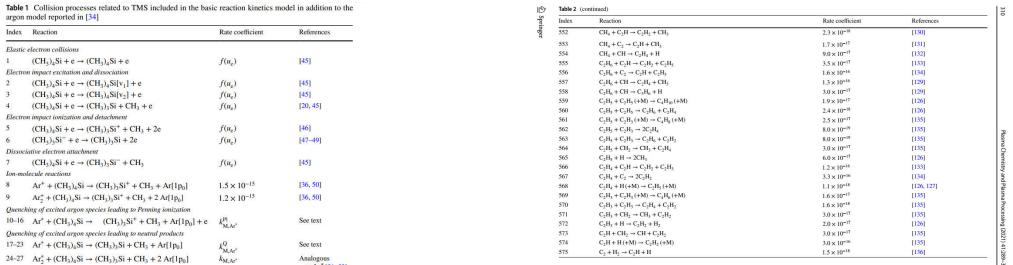

**Table 1** Collision processes related to TMS included in the basic reaction kinetics model in addition to the argon model reported in [34]

| Index | Reaction | Rate coefficient | References |
|---|---|---|---|
| *Elastic electron collisions* | | | |
| 1 | $(CH_3)_3Si + e \rightarrow (CH_3)_3Si + e$ | $f(u_{\varepsilon})$ | [45] |
| *Electron impact excitation and dissociation* | | | |
| 2 | $(CH_3)_3Si + e \rightarrow (CH_3)_3Si[v_1] + e$ | $f(u_{\varepsilon})$ | [45] |
| 3 | $(CH_3)_3Si + e \rightarrow (CH_3)_3Si[v_1] + e$ | $f(u_{\varepsilon})$ | [45] |
| 4 | $(CH_3)_3Si + e \rightarrow (CH_3)_3Si + CH_3 + e$ | $f(u_{\varepsilon})$ | [20, 45] |
| *Electron impact ionization and detachment* | | | |
| 5 | $(CH_3)_3Si + e \rightarrow (CH_3)_3Si^+ + CH_3 + 2e$ | $f(u_{\varepsilon})$ | [46] |
| 6 | $(CH_3)_3Si^- + e \rightarrow (CH_3)_3Si + 2e$ | $f(u_{\varepsilon})$ | [47–49] |
| *Dissociative electron attachment* | | | |
| 7 | $(CH_3)_3Si + e \rightarrow (CH_3)_2Si^- + CH_3$ | $f(u_{\varepsilon})$ | [45] |
| *Ion-molecule reactions* | | | |
| 8 | $Ar^+ + (CH_3)_3Si \rightarrow (CH_3)_3Si^+ + CH_3 + Ar[1p_k]$ | $1.5 \times 10^{-15}$ | [36, 50] |
| 9 | $Ar_2^+ + (CH_3)_3Si \rightarrow (CH_3)_3Si^+ + CH_3 + 2\,Ar[1p_k]$ | $1.2 \times 10^{-15}$ | [36, 50] |
| *Quenching of excited argon species leading to Penning ionization* | | | |
| 10–16 | $Ar^* + (CH_3)_3Si \rightarrow \quad (CH_3)_3Si^+ + CH_3 + Ar[1p_k] + e$ | $k_{M,Ar^*}^{PI}$ | See text |
| *Quenching of excited argon species leading to neutral products* | | | |
| 17–23 | $Ar^* + (CH_3)_3Si \rightarrow (CH_3)_3Si + CH_3 + Ar[1p_k]$ | $k_{M,Ar^*}^{Q}$ | See text |
| 24–27 | $Ar_2^* + (CH_3)_3Si \rightarrow (CH_3)_3Si + CH_3 + 2\,Ar[1p_k]$ | $k_{M,Ar^*}$ | Analogous to $Ar^*$ [51, 52] |



**Table 2** (continued)

| Index | Reaction | Rate coefficient | References |
|---|---|---|---|
| 552 | $CH_4 + C_2H \rightarrow C_2H_2 + CH_3$ | $2.3 \times 10^{-10}$ | [130] |
| 553 | $CH_4 + C_2 \rightarrow C_2H + CH_3$ | $1.7 \times 10^{-11}$ | [131] |
| 554 | $CH_4 + CH \rightarrow C_2H_4 + H$ | $9.0 \times 10^{-11}$ | [132] |
| 555 | $C_2H_4 + C_2H \rightarrow C_2H_3 + C_2H_2$ | $3.5 \times 10^{-11}$ | [133] |
| 556 | $C_2H_4 + C_2 \rightarrow C_2H + C_2H_3$ | $1.6 \times 10^{-14}$ | [134] |
| 557 | $C_2H_4 + CH \rightarrow C_2H_4 + CH_2$ | $1.3 \times 10^{-11}$ | [129] |
| 558 | $C_2H_4 + CH \rightarrow C_3H_4 + H$ | $3.0 \times 10^{-11}$ | [129] |
| 559 | $C_2H_4 + C_2H_2 (+M) \rightarrow C_4H_{6-8} (+M)$ | $1.9 \times 10^{-17}$ | [126] |
| 560 | $C_2H_4 + C_2H_3 \rightarrow C_2H_3 + C_2H_4$ | $2.4 \times 10^{-16}$ | [126] |
| 561 | $C_2H_4 + C_2H_3 (+M) \rightarrow C_4H_7 (+M)$ | $2.5 \times 10^{-17}$ | [135] |
| 562 | $C_2H_5 + C_2H_3 \rightarrow 2C_2H_4$ | $8.0 \times 10^{-16}$ | [135] |
| 563 | $C_2H_5 + C_2H_3 \rightarrow C_2H_4 + C_2H_2$ | $8.0 \times 10^{-16}$ | [135] |
| 564 | $C_2H_5 + CH_3 \rightarrow C_3H_4 + C_2H_4$ | $3.0 \times 10^{-13}$ | [135] |
| 565 | $C_2H_5 + H \rightarrow 2CH_3$ | $6.0 \times 10^{-11}$ | [126] |
| 566 | $C_2H_5 + C_2H \rightarrow C_2H_2 + C_2H_5$ | $1.2 \times 10^{-10}$ | [133] |
| 567 | $C_2H_5 + C_2 \rightarrow 2C_2H_2$ | $3.3 \times 10^{-16}$ | [134] |
| 568 | $C_2H_6 + H (+M) \rightarrow C_2H_5 (+M)$ | $1.1 \times 10^{-14}$ | [126, 127] |
| 569 | $C_2H_6 + C_2H_3 (+M) \rightarrow C_4H_9 (+M)$ | $1.6 \times 10^{-17}$ | [135] |
| 570 | $C_2H_6 + C_2H_3 \rightarrow C_2H_4 + C_2H_5$ | $1.6 \times 10^{-14}$ | [135] |
| 571 | $C_2H_6 + CH_3 \rightarrow CH_4 + C_2H_5$ | $3.0 \times 10^{-17}$ | [135] |
| 572 | $C_2H_7 + H \rightarrow C_2H_6 + H_2$ | $2.0 \times 10^{-17}$ | [126] |
| 573 | $C_3H + CH_3 \rightarrow CH + C_4H_6$ | $3.0 \times 10^{-11}$ | [135] |
| 574 | $C_3H + H (+M) \rightarrow C_3H_2 (+M)$ | $3.0 \times 10^{-16}$ | [135] |
| 575 | $C_3 + H_2 \rightarrow C_3H + H$ | $1.5 \times 10^{-14}$ | [136] |



*D. Loffhagen et al., Plasma Chem. Plasma Process.* **41** (2021) 289

- Chemical reactions in plasma model usually lead to stiff system of equations.

- Time scale of the problem spans from picoseconds to tens of seconds.

# FEDM (Finite Element Discharge Modelling) code

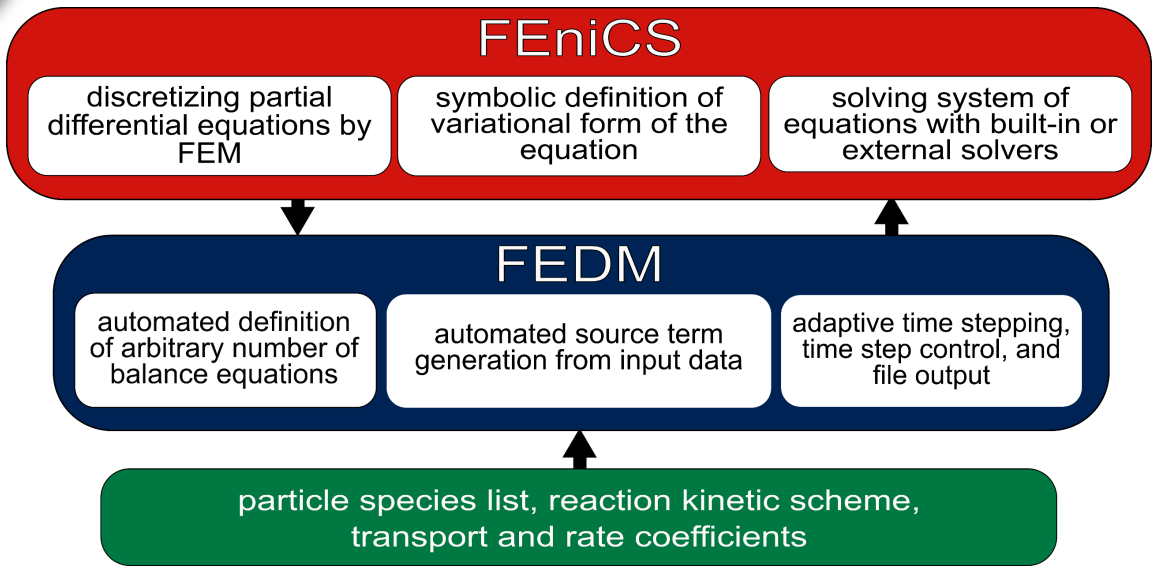

# FEDM (Finite Element Discharge Modelling) code

- Transport and reaction rate coefficients are imported into model in form of functions or look-up tables.
- Source term definition is automated based on the reaction kinetic scheme.
- Time discretization is done using backward differentiation formula.

$$y_{n+2} - \frac{(1+\omega_{n+1})^2}{1+2\omega_{n+1}} y_{n+1} + \frac{\omega_{n+1}^2}{1+2\omega_{n+1}} y_n = \Delta t_{n+2} \frac{1+\omega_{n+1}}{1+2\omega_{n+1}} f_{n+2}$$

- Time stepping control is done using either *H*211*b* or PI.3.4 controllers.

$$\Delta t_{n+1} = \left(\frac{0.8TOL}{\hat{r}_{n+1}}\right)^{0.3/k} \left(\frac{\hat{r}_n}{\hat{r}_{n+1}}\right)^{0.4/k} \Delta t_n$$

$$\Delta t_{n+1} = \left(\frac{0.8TOL}{\hat{r}_n}\right)^{0.25/k} \left(\frac{0.8TOL}{\hat{r}_{n-1}}\right)^{0.25/k} \left(\frac{\Delta t^n}{\Delta t^{n-1}}\right)^{-0.25} \Delta t^n$$

*E. Alberdi Celaya et al., Procedia Comput. Sci.,* ***29****, 1014–1026 (2014)*
*G. Söderlind and L. Wang, J. Comput. Appl. Math.,* ***185,*** *225–243 (2006)*
*G. Söderlind, Numer. Algorithms,* ***31****, 281–310 (2002)*

# Code verification by benchmarking

- Axisymmetric positive streamer in air at atmospheric pressure and 300 K is modelled using 2D FEDM code.
- Square domain has radius and gap distance of 1.25 cm.
- Background electric field is 15 kV/cm.
- Gaussian seed near the powered electrode is introduced to locally enhance the field and initiate the streamer.
- Mesh is refined towards the axis and streamer region (approx. 500000 elements).
- Linear Lagrange elements are used for all the equations.
- Time-step size is constant: Δt = 5 ps.
- Temporal evolution is followed up to 12 ns (2400 time steps).

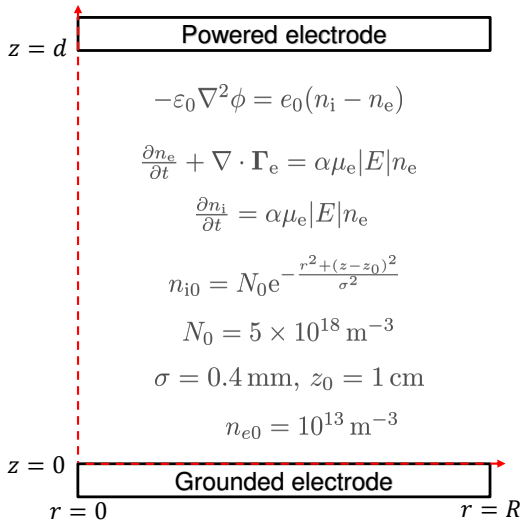


*B. Bagheri et al., Plasma Sources Sci. Technol.* ***27*** *(2018) 095002*

# Code verification by benchmarking

- Axisymmetric positive streamer in air at atmospheric pressure and 300 K is modelled using 2D FEDM code.
- Square domain has radius and gap distance of 1.25 cm.
- Background electric field is 15 kV/cm.
- Gaussian seed near the powered electrode is introduced to locally enhance the field and initiate the streamer.
- Mesh is refined towards the axis and streamer region (approx. 500000 elements).
- Linear Lagrange elements are used for all the equations.
- Time-step size is constant: Δt = 5 ps.
- Temporal evolution is followed up to 12 ns (2400 time steps).

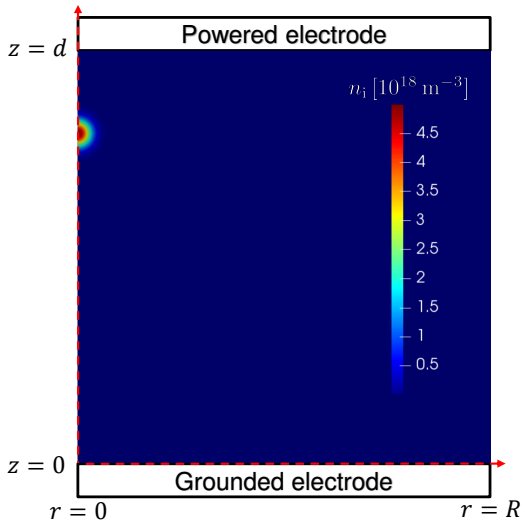


*B. Bagheri et al., Plasma Sources Sci. Technol.* ***27*** *(2018) 095002*

# Code verification by benchmarking

- Axisymmetric positive streamer in air at atmospheric pressure and 300 K is modelled using 2D FEDM code.
- Square domain has radius and gap distance of 1.25 cm.
- Background electric field is 15 kV/cm.
- Gaussian seed near the powered electrode is introduced to locally enhance the field and initiate the streamer.
- Mesh is refined towards the axis and streamer region (approx. 500000 elements).
- Linear Lagrange elements are used for all the equations.
- Time-step size is constant: Δt = 5 ps.
- Temporal evolution is followed up to 12 ns (2400 time steps).

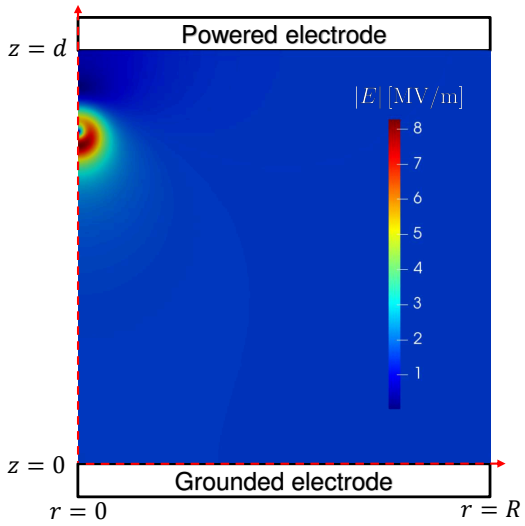


*B. Bagheri et al., Plasma Sources Sci. Technol.* ***27*** *(2018) 095002*

# Code verification by benchmarking

- Axisymmetric positive streamer in air at atmospheric pressure and 300 K is modelled using 2D FEDM code.
- Square domain has radius and gap distance of 1.25 cm.
- Background electric field is 15 kV/cm.
- Gaussian seed near the powered electrode is introduced to locally enhance the field and initiate the streamer.
- Mesh is refined towards the axis and streamer region (approx. 500000 elements).
- Linear Lagrange elements are used for all the equations.
- Time-step size is constant: Δt = 5 ps.
- Temporal evolution is followed up to 12 ns (2400 time steps).

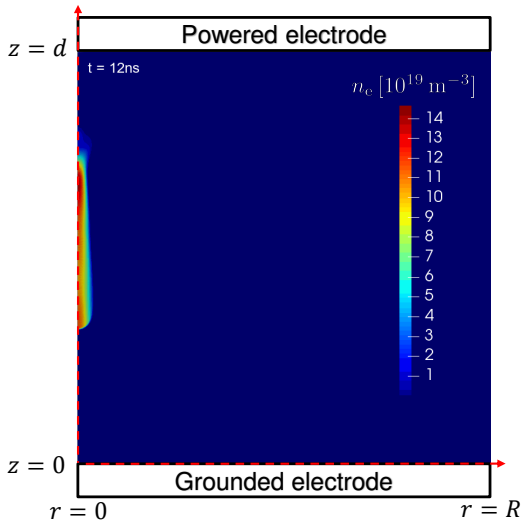


*B. Bagheri et al., Plasma Sources Sci. Technol.* ***27*** *(2018) 095002*

# Code verification by benchmarking

- Axisymmetric positive streamer in air at atmospheric pressure and 300 K is modelled using 2D FEDM code.
- Square domain has radius and gap distance of 1.25 cm.
- Background electric field is 15 kV/cm.
- Gaussian seed near the powered electrode is introduced to locally enhance the field and initiate the streamer.
- Mesh is refined towards the axis and streamer region (approx. 500000 elements).
- Linear Lagrange elements are used for all the equations.
- Time-step size is constant: $\Delta t = 5$ ps.
- Temporal evolution is followed up to 12 ns (2400 time steps).

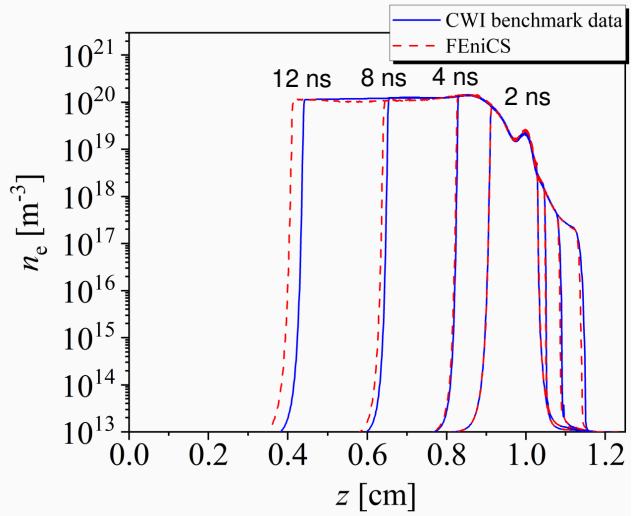


*B. Bagheri et al., Plasma Sources Sci. Technol.* ***27*** *(2018) 095002*

# Code verification by benchmarking

- Axisymmetric positive streamer in air at atmospheric pressure and 300 K is modelled using 2D FEDM code.
- Square domain has radius and gap distance of 1.25 cm.
- Background electric field is 15 kV/cm.
- Gaussian seed near the powered electrode is introduced to locally enhance the field and initiate the streamer.
- Mesh is refined towards the axis and streamer region (approx. 500000 elements).
- Linear Lagrange elements are used for all the equations.
- Time-step size is constant: $\Delta t = 5$ ps.
- Temporal evolution is followed up to 12 ns (2400 time steps).

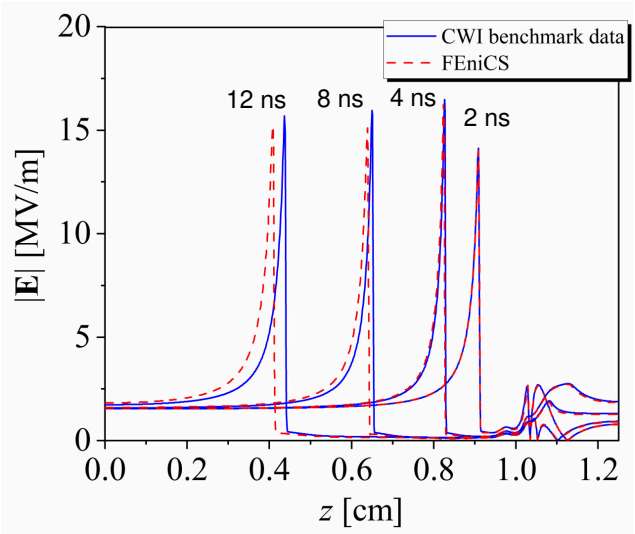


*B. Bagheri et al., Plasma Sources Sci. Technol.* ***27*** *(2018) 095002*

# Dielectric barrier discharge (DBD) modelling

- Atmospheric-pressure DBD in argon in asymmetric configuration is modelled using 2D FEDM code.
- Electrodes of radius 2 mm are set 1.5 mm apart.
- Grounded electrode (top) is covered by 0.5 mm thick dielectric.
- Pulsed voltage is applied to powered electrode (bottom).
- Gaussian seed near the powered electrode is introduced to locally enhance the field and initiate the streamer.
- Mesh is refined near the streamer region and along the dielectric (approx. 350000 elements).
- Linear Lagrange elements are used for all the equations.
- Adaptive time stepping is used (1 ps < Δt < 100 ps).
- Temporal evolution is followed up to about 43 ns.

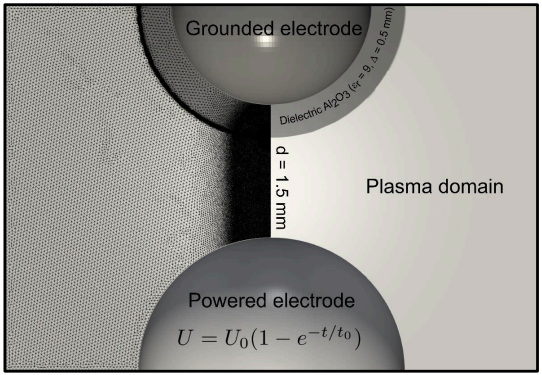

# Dielectric barrier discharge (DBD) modelling

- Atmospheric-pressure DBD in argon in asymmetric configuration is modelled using 2D FEDM code.
- Electrodes of radius 2 mm are set 1.5 mm apart.
- Grounded electrode (top) is covered by 0.5 mm thick dielectric.
- Pulsed voltage is applied to powered electrode (bottom).
- Gaussian seed near the powered electrode is introduced to locally enhance the field and initiate the streamer.
- Mesh is refined near the streamer region and along the dielectric (approx. 350000 elements).
- Linear Lagrange elements are used for all the equations.
- Adaptive time stepping is used (1 ps < Δt < 100 ps).
- Temporal evolution is followed up to about 43 ns.

$$-\varepsilon_0 \varepsilon_\mathrm{r} \nabla^2 \phi = \sum_p q_p n_p$$

$$\frac{\partial n_p}{\partial t} + \nabla \cdot \mathbf{\Gamma}_p = S_p$$

$$\frac{\partial w_\mathrm{e}}{\partial t} + \nabla \cdot \mathbf{Q}_\mathrm{e} = -e_0 \mathbf{E} \cdot \mathbf{\Gamma}_\mathrm{e} + \widetilde{S}_\mathrm{e}$$

$$\frac{\partial \sigma}{\partial t} = \sum_p q_p \mathbf{\Gamma}_p \cdot \boldsymbol{\nu}$$

# Dielectric barrier discharge (DBD) modelling

- Atmospheric-pressure DBD in argon in asymmetric configuration is modelled using 2D FEDM code.
- Electrodes of radius 2 mm are set 1.5 mm apart.
- Grounded electrode (top) is covered by 0.5 mm thick dielectric.
- Pulsed voltage is applied to powered electrode (bottom).
- Gaussian seed near the powered electrode is introduced to locally enhance the field and initiate the streamer.
- Mesh is refined near the streamer region and along the dielectric (approx. 350000 elements).
- Linear Lagrange elements are used for all the equations.
- Adaptive time stepping is used (1 ps < Δt < 100 ps).
- Temporal evolution is followed up to about 43 ns.

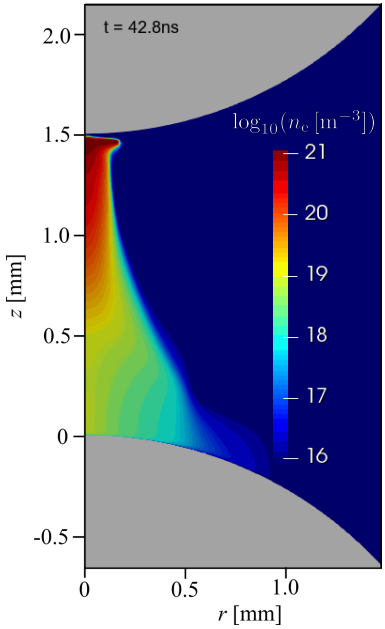

# Conclusion and outlook

- FEDM code for automated set-up of the equations is developed.
- The code is verified using benchmarking.
- The challenges in cases where the problem is defined on several subdomains, such as DBDs, could possibly be resolved using mixed-dimensional formulation.
- Handling of electron-energy-dependent and electric-field-dependent coefficients should be further addressed because they can lead to small time-step sizes.

# Contact


Leibniz Institute for Plasma Science and Technology
Address: Felix-Hausdorff-Str. 2, 17489 Greifswald
Phone: +49 - 3834 - 554 3911, Fax: +49 - 3834 - 554 301
E-mail: aleksandar.jovanovic@inp-greifswald.de, Web: www. leibniz-inp.de